

УДК 616.72-089.843:[615.465:669.056.91-022.513.6

## Examination of surface and material properties of nanostructural oxide coatings for joint total and module replacement arthroplasty

A. Zykova<sup>1</sup>, V. Safonov<sup>1</sup>, J. Smolik<sup>2</sup>, R. Rogowska<sup>2</sup>,  
V. Lukyanchenko<sup>3</sup>, A. Samoilenko<sup>4</sup>, N. Donkov<sup>5</sup>,  
D. A. Kolesnikov<sup>6</sup>, I. Yu. Goncharov<sup>6</sup>

<sup>1</sup> National Science Centre «Kharkov Institute of Physics and Technology», Kharkov. Ukraine

<sup>2</sup> Institute for Sustainable Technologies, National Research Institute, Radom. Poland

<sup>3</sup> Inmasters Ltd, Kharkov. Ukraine

<sup>4</sup> Lugansk State Medical University, Lugansk. Ukraine

<sup>5</sup> Institute of Electronic Bulgarian Academy of Sciences, Sofia. Bulgaria

<sup>6</sup> Belgorod National State University, Belgorod. Russia

*Deposition of functional coatings on metal substrates (stainless steel 1H18N9, titanium alloy Ti6Al4V) makes it possible to combine biocompatibility of ceramics with advantages of metals for improving tribological characteristics of prostheses and creating new low-cost and innovative prototypes for defect replacement in patients of different age groups. The specific properties of nanostructural oxide coatings make them most promising for subsequent applications in implantology. High hardness parameters up to 9 Gpa, adhesion strength up to 40 N and a low friction coefficient with a strong tendency to decrease in fluids (0.07) were estimated. The corrosion test results show that oxide coating deposition had improved the corrosion resistance parameters by a factor of ten both for stainless steel and titanium substrates. The surface with oxide coatings demonstrated electrical inertness and capacitive properties. The hydrophilic property of coated surfaces versus the metal one was investigated by the method of tensiometry. Surfaces with nanostructural oxide coatings demonstrated improved biocompatibility due to dielectric properties and high values of surface energy.*

*Нанесение функциональных покрытий на металлические материалы (нержавеющая сталь 1H18N9, сплав титана Ti6Al4V) позволяет совмещать биосовместимость керамики с преимуществами металлов для усовершенствования трибологических характеристик протезов и создания недорогих инновационных прототипов с целью замещения дефектов у пациентов различных возрастных групп. Специфические свойства наноструктурных оксидных покрытий делают их наиболее перспективными для дальнейшего применения в имплантологии. Были исследованы высокие показатели твердости порядка 9 ГПа, адгезионной прочности порядка 40 Н и низкий коэффициент трения с выраженной тенденцией к уменьшению в жидкостях порядка 0,07. Результаты коррозионных тестов демонстрируют улучшение на порядок сопротивленности коррозии как для субстратов из нержавеющей стали, так и сплава титана. Поверхность с оксидными покрытиями демонстрирует электрическую инертность и емкостные свойства. Гидрофильность поверхности покрытий в сравнении с металлическими субстратами исследована методом тензиометрии. Поверхности с наноструктурными оксидными покрытиями обладают улучшенной биосовместимостью благодаря диэлектрическим свойствам и высоким значениям поверхностной энергии.*

**Key words:** arthroplasty, implant materials, nanostructural oxide coatings, corrosion resistance, biocompatibility

## Introduction

Promising results of total and module joints replacement were widely adopted for patients of different age groups. In order to improve the results of subsequent arthroplasty, still more interest is paid to the use of alternative bearing surfaces and implementation of new advanced materials and technologies. It takes some time and needs long-term clinical studies to assess the effectiveness of new implant construction and material applications.

Oxide ceramic parts are widely used in ceramic ball bearings. Their higher hardness means that they are much less susceptible to wear and can offer more than triple lifetimes. They also deform less under load; it means they have less contact with the bearing retainer walls and can roll faster. In some applications, heat from friction during rolling can cause problems for metal bearings, these problems being reduced by use of ceramics. Ceramics are also more chemically resistant and can be used in wet environments, where steel bearings would rust. In many cases, their electrical insulating properties may also be valuable in bearings.

The total and module replacement of hip, shoulder, knee and elbow joints is one of the most successful and effective surgical operations in modern medical practice [1, 2]. The long-term experience of different patient group investigations demonstrates high survival parameters under medical observations over 20–30 years. A serious problem of cyclic mechanical loads of prosthesis coupling and accelerated friction element destruction due to the patient's motion activity [3–7] is arising. There is a direct effect of wearing rate of artificial joint on subsequent osteolytic processes, aseptic loosening and need of revision operations. Recently the advancement of already existing joint sliding coupling characteristics (metal-metal, metal-ceramic, ceramic-ceramic couples) and search for alternative materials (metal, ceramic, coatings) have become the main directions in the improvement of tribological parameters of joints [8–10]. In main cases of metal-on-metal couple applications, a mixed lubrication of friction surfaces takes place. A hydrodynamic (liquid) lubrication exists in cases of large diameters of the heads. The use of ceramic materials makes it possible to improve wettability characteristics of joints and fluid friction conditions [11]. Ceramic materials have high hardness and wear resistance parameters, biocompatibility in comparison with metal elements, but there is a risk of brittle failure of ceramic heads [12, 13]. Other negative results of metal and ceramic material application include accumulation of toxic wear debris in the surrounding implant tissues and subsequent dissemination of wear particles to the visceral organs: liver, spleen,

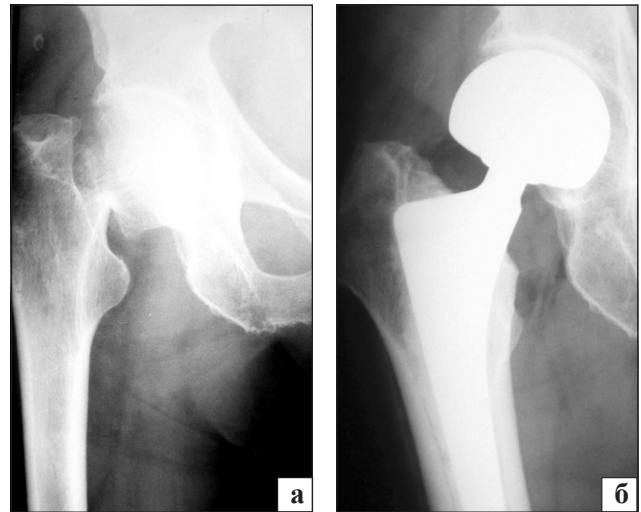


**Fig. 1.** Radiographs of the clinic application of module hip joints with ceramic oxide coatings

kidneys [14–17]. Nanostructural coatings based on Al, Zr, Ti oxides exhibit unique properties [18–20]: high inductivity, density, bio- and chemical inertness, which are very important for subsequent implant and tissue engineering applications. Corrosion is one of the major processes that cause problems when metals and alloys are used as implants in the body [21, 22]. The functional coating deposition on metal substrates (stainless steel 1H18N9, titanium Ti6Al4V and zirconium alloys) makes it possible to combine the biocompatibility of ceramic materials with fracture toughness and failure strength of metals for subsequent advancing of joint tribological characteristics and creation of new prototypes of low-cost and innovative hip, shoulder, knee and elbow joints for different age groups (fig. 1).

## Materials and methods

The substrates for deposited coatings were the popular implant materials such as stainless steel (1H18N9) and titanium-based material (Ti4Al6V) samples. The substrates were cleaned in an ultrasonic bath following the standard technology. Nanostructural  $\text{Al}_2\text{O}_3$  (MS) magnetron sputtering deposition was performed in a high vacuum pumping system with the base pressure of about 10–15 mBar. The main details of the magnetron and ion source in the sputtering chamber were demonstrated before [23]. The magnetron discharge power was 1–4 kW, the power of activated oxygen source up to 1 kW, the coating deposition rate 8  $\mu\text{m}/\text{hour}$ . There was a problem of target oxidation during deposition process. In excessive oxygen flow conditions the process shifted to the target passivation regimen (the lower part of volt-ampere characteristic (VAC) curves, fig. 2). The sputtering process should be made in the regimens far from the target passivation

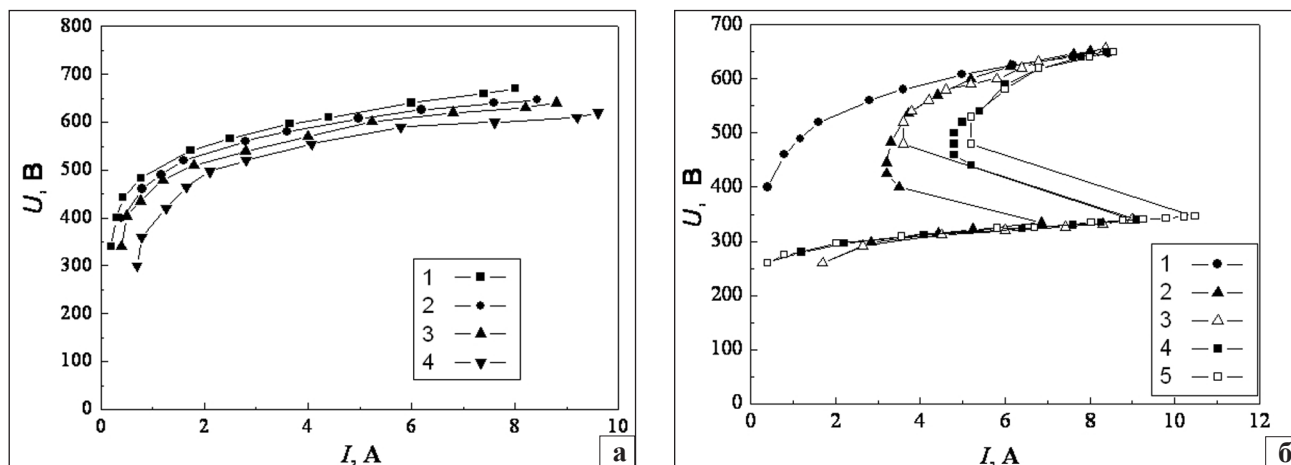


**Fig. 2.** Volt-ampere characteristics of magnetron discharge in argon. a) Ar pressure was  $1-5 \cdot 10^{-4}$  Pa,  $2-6 \cdot 10^{-2}$  Pa,  $3-8 \cdot 10^{-2}$  Pa,  $4-2.5 \cdot 10^{-1}$  Pa. b) In argon with oxygen: Ar pressure was  $6 \cdot 10^{-2}$  Pa and oxygen flow  $1-q$  0 cm<sup>3</sup>/min,  $2,3-q$  17 cm<sup>3</sup>/min,  $4,5-q$  26 cm<sup>3</sup>/min for aluminum target material

for subsequent aluminum oxide coating deposition with a high stoichiometric composition. Also, such deposition conditions make it possible to avoid the formation of micro-arcs and micro-drops, which increase corrosion resistance properties. The optimum conditions were realized for the upper part of VAC curves of magnetron discharge in argon with oxygen (fig. 2 a, b).

The structure of Al<sub>2</sub>O<sub>3</sub> (MS) magnetron sputtered films was investigated by means of XPS and XRD methods. X-ray diffraction profiles of Al<sub>2</sub>O<sub>3</sub> (MS) were observed by means of diffraction device «DRON-3» with filtered Cu-K $\alpha$  radiation. X-ray photoelectron spectroscopy was carried out using ESCALAB MkII (VG Scientific) electron spectrometer at a base pressure in the analysis chamber of  $5 \times 10^{-10}$  mbar (during the measurement  $1 \times 10^{-8}$  mbar), using AlK $\alpha$

X-ray source (excitation energy  $h\nu = 1,486.6$  eV). The instrumental resolution was measured as the full width at a half maximum (FWHM) of Ag3d<sub>5/2</sub>, the photoelectron peak was 1 eV. The coating thickness, hardness and elastic modulus were evaluated by standard methods [23]. Adhesion parameters and friction coefficients were measured by Scratch method within the load range of 0–200 N.

The surface topography and roughness were estimated by profilometer Hommel T-2000 measurements and by AFM. The surface free energy (SFE), polar and dispersion components were determined by means of Wu and Owens-Wendt-Rabel-Kaelble methods.

Corrosion tests by the potentiodynamic method, Tafel and Stern curves were made by Potentiostat PARSTAT 2263 (AMETEK, USA). Corrosion examinations of anodic polarization at the potential range of  $-1.0$  V... $+2.0$  V with scanning rate 1 mV/s, Tafel  $-0.050$  V... $+0.050$  V and Stern  $-0.020$  V... $+0.020$  V range curves at 0.5 N NaCl and SBF (NaCl<sub>0</sub>-8,035,

NaHCO<sub>3</sub>-0,355, KCl-0,225, K<sub>2</sub>HPO<sub>4</sub> 3H<sub>2</sub>O-0,231, MgCl<sub>2</sub> 6H<sub>2</sub>O-0,311, CaCl<sub>2</sub>-0,292, Na<sub>2</sub>SO<sub>4</sub>-0,072) at pH = 7.4 and temperature of 37 °C in solutions were carried out. Surface morphology was investigated by means of Interferometric Microscope Talysurf CCI (Taylor Hobson), SEM and AFM (Quesant Instrument Corporation, USA) methods.

Cytotoxicity and cytocompatibility were evaluated at in vitro tests. In the process of cell cultivation (fibroblasts) with coated and uncoated samples, cell cytology, morphology and vital capacity were determined after 24 h and 3, 5 days of cultivation. Rat hypodermic cellular tissue was extracted for obtaining an initial fibroblast culture. The suspension of extracted cells was centrifuged at 750 r. p. m. during 15 min. The culturing cell area density was  $3 \times 10^5$  cell/ml. Fibroblast cultivation in 3 ml of Dulbecco Modified Eagle's Medium (DMEM, Sigma) supplemented with 10 % fetal calf serum (FCS), 80 mg/ml penicillin, 100 mg/ml streptomycin was made by methods of monolayer culture at thermostat condition (temperature 37 °C in 5 % CO<sub>2</sub> atmosphere during 5 days). The cells, adhered on the samples, were cleaned by a buffer solution (pH 7.2) and double distilled water and fixed at 2.5 % glutaraldehyde on a 0.1 M buffer solution during 2 h and 1 % OsO<sub>4</sub> solution during 1 h. Then the samples were dehydrated at a certain concentration of alcohol. Other samples with the adhered cells were trypsinized with 0.01 % trypsin/0.5 mM EDTA. The experiments were independently triplicated. The analysis of cell adhesion on substrates was made by means of SEM and AFM methods.

## Results and discussion

The structure of Al<sub>2</sub>O<sub>3</sub> (MS) thin films was investigated by means of XPS and XRD methods. X-ray diffraction profiles of Al<sub>2</sub>O<sub>3</sub> (MS) as deposited coatings

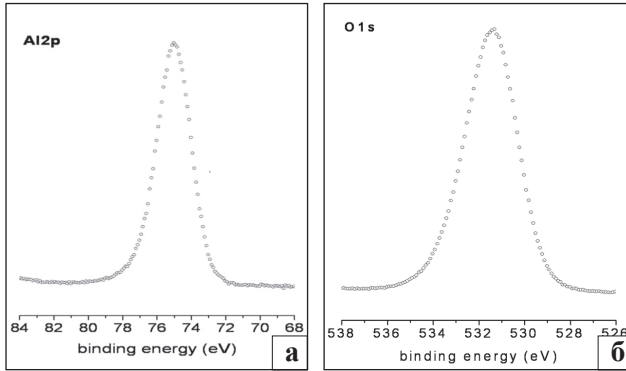


**Fig. 3.** Al2p XPS spectra of Al<sub>2</sub>O<sub>3</sub> (MS) coatings (a), O1s XPS spectra of Al<sub>2</sub>O<sub>3</sub> (MS) coatings (b)

demonstrated an amorphous nature, no peaks were observed. The structural analysis of Al<sub>2</sub>O<sub>3</sub> (MS) oxide coatings by means of XPS method also was made (fig. 3). The photoelectron spectra of Al2p, O1s and C1s spectra were observed and confirmed a strong Al<sub>2</sub>O<sub>3</sub> oxide stoichiometric composition.

The surface structure, morphology and topography of deposited oxide coatings were estimated by AFM (fig. 4).

The coatings underwent mechanical testing. Their thickness, hardness, adhesion parameters and elastic modulus were measured by standard tests. Al<sub>2</sub>O<sub>3</sub> coatings were scratched with the Rockwell indenter with the tip radius of 200 μm, within the load range of 0–200 N, obtained on uncoated steel substrates.

Typical scratch-test results for Al<sub>2</sub>O<sub>3</sub> films are presented in fig. 5 a versus a scratch test of a TiN coating (fig. 5 b).

The friction coefficient of oxide coatings was about 0.1, it being less than for metal materials and nitride coatings and having a strong tendency to decrease in fluids (0.07).

Corrosion parameters of Al<sub>2</sub>O<sub>3</sub> oxide coatings deposited on stainless steel (H18N9) and titanium-based material (Ti4Al6V) samples were analysed. The samples were immersed in an electrolyte and their potential was monitored as a function of time until the potential reached a stable value. Corrosion tests (in SBF solutions) of anodic polarization by potentiodynamic method at the potential range of –1.0V...+2.0 V with the scanning rate of 1 mV/s were presented in fig. 6 for SS, SS/Al<sub>2</sub>O<sub>3</sub> and Ti, Ti/Al<sub>2</sub>O<sub>3</sub> coatings.

The data show that deposition of the coatings improved corrosion resistance parameters by a factor of ten and charge-transfer kinetic performance of interfaces both for stainless steel and titanium substrates.

Surface topography and corrosion failure of uncoated metal substrates after corrosion tests in simulated body fluids (SBF) were investigated by means of Interferometric Microscope Talysurf CCI (Taylor

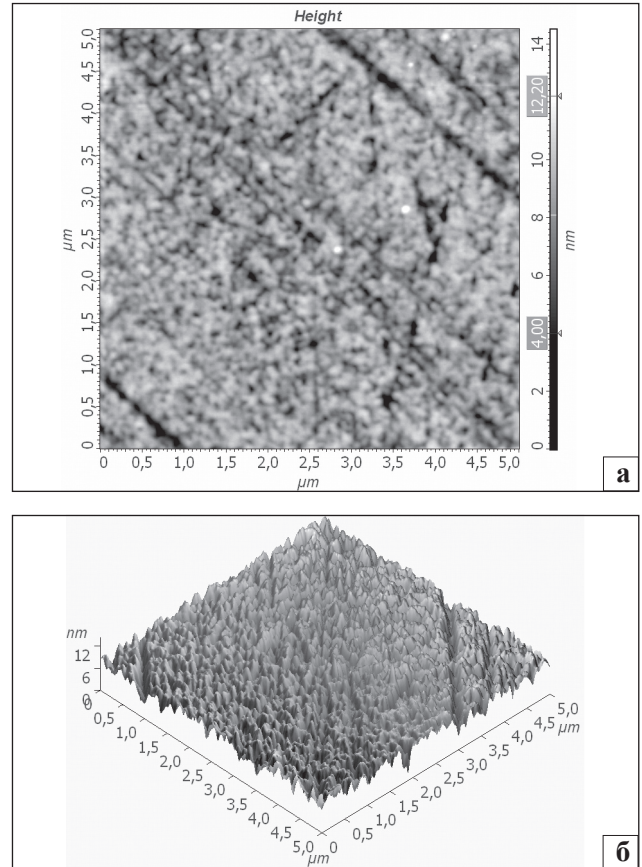


**Fig. 4.** The surface structure of Al<sub>2</sub>O<sub>3</sub> coatings by AFM

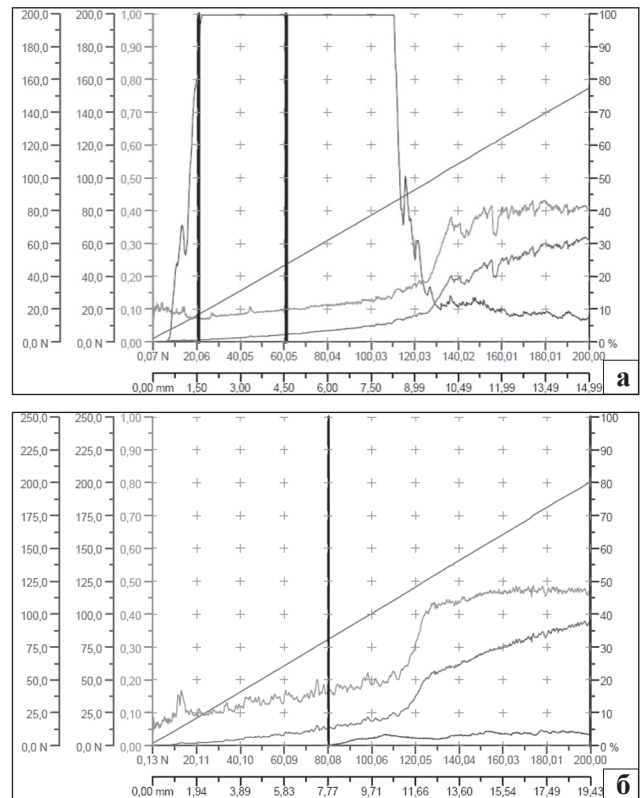


**Fig. 5.** Adhesion and friction coefficient test results for 2.9 μm Al<sub>2</sub>O<sub>3</sub> film (a) versus a scratch test of 2.8 μm TiN coating (b)

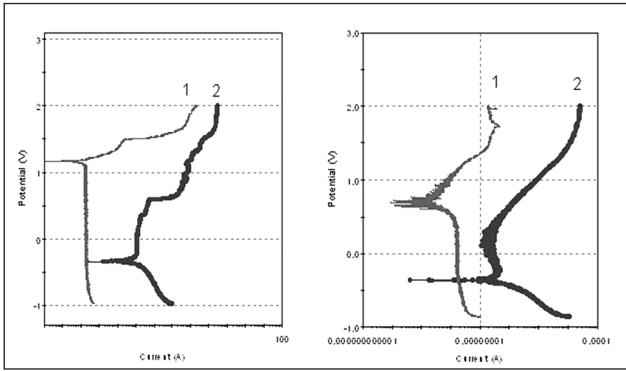


**Fig. 6.** Anodic polarization curves for coatings in SBF solutions: a) SS/ $\text{Al}_2\text{O}_3$  — 1, SS — 2; b) Ti/ $\text{Al}_2\text{O}_3$  — 1, Ti — 2

Hobson) and AFM (Quesant Instrument Corporation, USA) methods (fig. 7).

The contact angles were measured by means of tensiometric method (table 1). Prior to contact angle measurements, samples were ultrasonically cleaned in acetone and deionized water and dried. Advancing contact angles were measured by Wilhelm's method (Kruss K12) at a temperature of 20 °C [23].

Such standard liquids with well-known values of surface tension, component of dispersion and polar interaction as water, formamide, diiodomethane, ethylene glycol and  $\alpha$ -bromo-naphthalene were used.

The surface free energy (SFE) and its polar and dispersion components were determined by means of Wu [24] (table 2) and Owens-Wendt-Rabel-Kaelble [25] methods.

Experiments to study cytotoxicity and cytocompatibility in vitro — in a culture of fibroblasts — were carried out. In the process of cell cultivation with coated samples, cell cytology, morphology and vitality were determined after 24 h and 3, 5 days of cultivation.

The data present the vital capacity of cells. After 3 days of culturing, fibroblasts were well spread both on the control and coated surfaces. Their morphology was typical for cells on coated surfaces. After 5

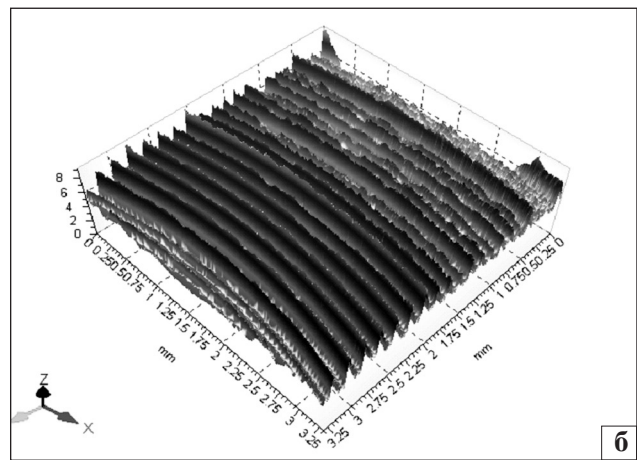
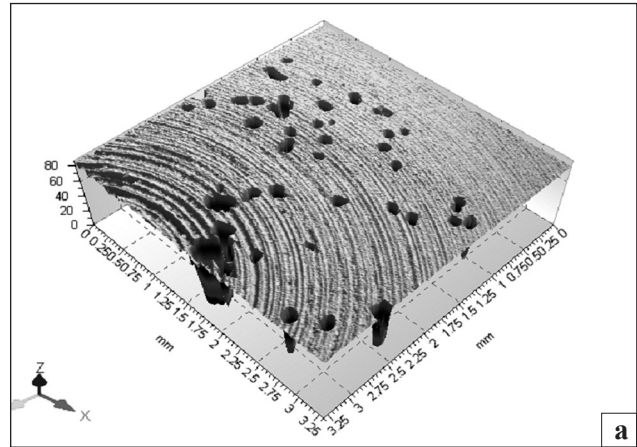


**Fig. 7.** Surface topography after corrosion tests in SBF solution by Interferometric Microscope Talysurf CCI (Taylor Hobson): a) 1H18N9T substrate material, b) Ti6Al4V substrate material

days of cultivation the density of cells increased in all samples. In the centre of each sample the density was maximal. Differences in cell attachment (the number of detached cells) and spreading on various surfaces were detected (fig. 8).

The best biological response parameters (cell number, morphology, vital capacity) were obtained in the case of substrates with the most optimum parameters

**Table 1.** Average values of the advancing contact angle at 20 °C temperature

Substrate/coating	Water, [°]	Formamide, [°]	Ethylene Glycole, [°]	Diio-dometane, [°]	$\alpha$ -bromo-naphthalen, [°]
Steel(SS)/ $\text{Al}_2\text{O}_3$	54,70	48,15	42,29	44,02	26,97
Ti6Al4V/ $\text{Al}_2\text{O}_3$	55,60	44,00	44,77	46,17	28,04
Steel(SS)	72,40	45,60	51,80	37,30	18,30

**Table 2.** The values of total surface free energy, dispersion and polar components (by Wu method for the formamide-water system at 20 °C temperature)

Substrate/coating	$\sigma$ [mN/m]	$\sigma^d$ [mN/m]	$\sigma^p$ [mN/m]
SS/ $\text{Al}_2\text{O}_3$	48,61	18,89	29,72
Ti6Al4V/ $\text{Al}_2\text{O}_3$	49,11	21,29	27,82
SS	43,25	26,95	16,30
Ti6Al4V	51,92	27,03	24,89

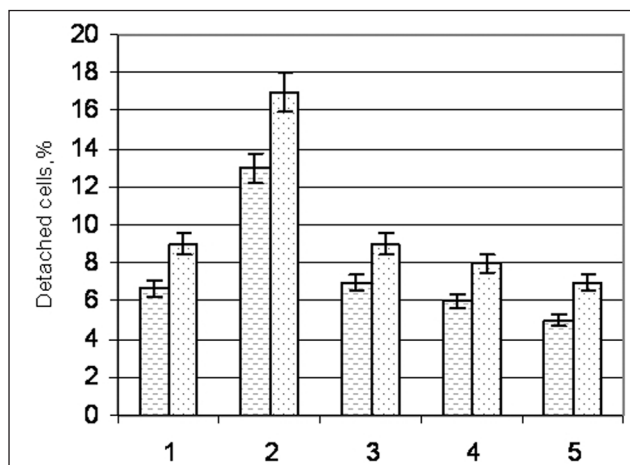


**Fig. 8.** The number of detached cells ( $P < 0.05$ ) on the surface of SS (AISI 321) and Ti4Al6V substrates with Al<sub>2</sub>O<sub>3</sub> (MS) coatings after 3 and 5 days of cultivation. 1 — control glass, 2 — SS, 3 — SS/Al<sub>2</sub>O<sub>3</sub>, 4 — Ti4Al6V, 5 — Ti4Al6V/Al<sub>2</sub>O<sub>3</sub>

of polar part component of SFE such as Ti4Al6V and oxide coatings Al<sub>2</sub>O<sub>3</sub> (MS) (table 2).

## Conclusions

The structure and mechanical, corrosion, adhesion properties of oxide coatings deposited on such load-bearing substrates as SS 1H18N9T and Ti6Al4V were studied. The XPS results demonstrate a strong Al<sub>2</sub>O<sub>3</sub> oxide stoichiometric composition of deposited coatings. Nanostructural surface parameters were observed by AFM. High hardness parameters up to 9 Gpa, adhesion strength up to 40 N and a low friction coefficient of oxide coatings, with a strong tendency to decrease in fluids (0.07), were obtained. The corrosion test results also show that oxide coating deposition improved corrosion resistance parameters by a factor of ten and charge-transfer kinetic performance of interfaces both for stainless steel and titanium substrates. The surface with nanostructural oxide coating has a strong capacitive response due to its electrical inert properties and high dielectric constants. The hydrophilic nature of coated surfaces versus the metal one was demonstrated in tensiometric tests (table 2). The best biological response parameters (total cell number, cell morphology and viability) were obtained in the case of oxide coatings on substrate materials (1H18N9, Ti6Al4V) with roughness parameters about 20–40 nm and the most optimum parameters of polar part component of SFE such as Ti4Al6V (24.9 mN/m) and oxide coatings Al<sub>2</sub>O<sub>3</sub> (MS) (29.7 mN/m) (fig. 8).

Stainless steel and titanium alloy implants with ceramic oxide coatings exhibited the best biocompatibility, remodelling process improvement and absence of inflammatory reactions on the bone-implant interface

versus uncoated samples. The clinical approbation of the advanced materials and coatings as promising biomaterials makes it possible to suggest principally new strategies for treating complicated diseases and developing modern biomedical methods [26].

## Literature

- Bohm E. R. Employment status and personal characteristics in patients awaiting hip-replacement surgery / E. R. Bohm // *Can. J. Surg.* — 2009. — Vol. 52, № 2. — P. 142–146.
- Morscher E. W. Failures and successes in total hip replacement Review / E. W. Morscher // *Scand. J. Surg.* — 2003. — Vol. 92. — P. 113–120.
- Mahomed N. N. Rates and outcomes of primary and revision total hip replacement in the United States medicare population / N. N. Mahomed // *J. Bone Joint Surg.* — 2003. — Vol. 85-A. — P. 27–32.
- Patient characteristics affecting the prognosis of total hip and knee joint arthroplasty: a systematic review / P. L. Santaguida G. A. Hawker, P. L. Hudak et al. // *Can. J. Surg.* — 2008. — Vol. 51, № 6. — P. 428–436.
- Petsatodis G. E. Primary cementless total hip arthroplasty with an alumina ceramic-on-ceramic bearing: results after a minimum of twenty years of follow-up / G. E. Petsatodis // *J. Bone Joint Surg.* — 2010. — Vol. 92-A, № 3. — P. 639–644.
- Lymphocyte proliferation responses in patients with pseudotumors following metal-on metal hip resurfacing arthroplasty / Y. M. Kwon, P. Thomas, B. Summer et al. // *J. Orthop. Res.* — 2010. — Vol. 28, № 4. — P. 444–450.
- Patient activity after total hip arthroplasty declines with advancing age / S. Kinkel et al. // *Clinic. Orthop.* — 2009. — Vol. 467, № 8. — P. 2053–2058.
- Campbell P. Histological features of pseudotumor-like tissues from metal-on-metal hips / P. Campbell // *Clinic. Orthop.* — 2010. — Vol. 468, № 9. — P. 2321–2327.
- Comparison of the cytotoxicity of clinically relevant cobalt-chromium and alumina ceramic wear particles in vitro / M. A. Germain et al. // *Biomaterials.* — 2003. — Vol. 24, № 3. — P. 469–479.
- Ceramic acetabular linear fracture in total hip arthroplasty with a ceramic sandwich cup / M. Hasegawa, A. Sudo, H. Hirata, A. Uchida // *J. Arthroplasty.* — 2003. — Vol. 18, № 5. — P. 658–661.
- Lee J. Y. Alumina-on-Polyethylene Bearing Surfaces in Total Hip Arthroplasty / J. Y. Lee, Sh.-Y. Kim // *Open Orthop. J.* — 2010. — Vol. 4. — P. 56–60.
- Clinical experience with ceramics in total hip replacement / Oonishi et al. // *Clinic. Orthop.* — 2000. — Vol. 379. — P. 77–84.
- Examination of surface and material properties of explanted zirconia femoral heads / E. M. Santos et al. // *J. Arthroplasty.* — 2004. — Vol. 19, № 7. — Suppl. 2. — P. 30–34.
- Metal wear particle characterization from metal-on-metal hip replacements: Transmission electron microscopy study of periprosthetic tissues and isolated particles / P. F. Doom et al. // *J. Biomed. Mater. Res.* — 1998. — Vol. 42. — P. 103–111.
- Merritt K. Distribution of cobalt chromium wear and corrosion products and biologic reactions / K. Merritt, S. A. Brown // *Clinic. Orthop.* — 1996. — Vol. 329. — P. 233–243.
- Dissemination of wear particles to the liver, spleen and abdominal lymph nodes of patients with hip or knee replacement / R. M. Urban et al. // *J. Bone Joint Surg.* — 2000. — Vol. 82-A. — P. 457–476.
- Willmann G. Ceramic femoral head retrieval data / G. Willmann // *Clinic. Orthop.* — 2000. — Vol. 379. — P. 22–28.
- Nanocomposite oxide and nitride hard coating produced by

- pulse magnetron sputtering / H. Klostermann, B. Bufcher, F. Fietzke et al. // *Surface&Coating Tech.* — 2005. — Vol. 200. — P. 760–764.
19. Direct current magnetron sputtering deposition of nanocomposite alumina-zirconia thin films / D. H. Trinh, T. Kubart, T. Nyberg et al. — *Thin Solid Films.* — 2008. — Vol. 516. — P. 8352–8358.
  20. The corrosion properties of zirconium and titanium load-bearing implant materials with protective oxide coatings [Электронный ресурс] / A. Zykova, V. Safonov, J. Smolik et al. // *Proceeding of 13th International Conference on Plasma Surface Engineering (September 10 — 14, 2012, Garmisch-Partenkirchen, Germany).* — Режим доступа: [http://www.pse-confeences.net/tl\\_files/pse2012/abstractupload/PSE2012-PO3048-ext.pdf](http://www.pse-confeences.net/tl_files/pse2012/abstractupload/PSE2012-PO3048-ext.pdf).
  21. Interactions between cells and titanium surfaces / E. Eisenbarth, D. Velten, K. Schenk-Meuser et al. // *Biomolecular Engineering.* — 2002. — Vol. 19. — P. 243–249.
  22. Physico-chemistry and cytotoxicity of ceramics / L. Dion, F. Bordenave, R. Lefebvre, C. V. Boreille // *Journal of Materials Science: Materials in Medicine.* — 1994. — P. 18–24.
  23. The influence of surface parameters of coatings deposited by various vacuum-plasma methods on the cell/material interaction in vitro tests / A. Zykova, V. Safonov, V. Luk'yanchenko et al. // *Problems of Atomic Science and Technology Series: Plasma Physics* — 2007. — Vol. 13 — P. 200–204.
  24. Wu S. J. Surface and interfacial tensions of polymer melts / S. J. Wu // *Phys. Chem.* — 1970. — Vol. 74. — P. 632.
  25. Owens D. K. Estimation of the surface free energy of polymers / D. K. Owens, R. C. Wendtn // *J. Appl. Polym. Sci.* — 1969. — Vol. 13. — P. 1741.
  26. Cell adhesion on biomaterial surfaces with nanocomposite oxide coatings / O. Vyrva, A. Zykova, V. Safonov et al. // *Orthopaedics, traumatology and prosthetics.* — 2011. — Vol. — P. 84–87.

Статья поступила в редакцию 18.01.2013